

Malicious UAV Detection Using Blind Source Separation Algorithm and Neural Network Classifier

K. Lakshmipriya¹, S.P. Charu Prafulla², S. Lokesh³, O. Uma Maheswari⁴

^{1,2,4}Department of Electronics and Communication Engineering, College of Engineering Guindy, Anna University, Chennai, India

³Ramanujan Computing Centre, College of Engineering Guindy, Anna University, Chennai, India

Abstract - Unmanned aerial vehicle(UAV) technology is the rapid growing technology in the field of monitoring for security purposes, pesticides spraying and various other applications. In the recent days, one of the major concerns is entering of malicious UAVs into the secured perimeter that might result in Drone-based cyberattacks. So, the detection of these malicious UAVs are crucial. In this work, an acoustic method of detecting malicious UAVs is proposed. The mixed form of the acoustic signals of two kinds of drones, namely, Fixed-wing and Multi- rotor are passed through the Blind Source Separation (BSS) block, where the kurtosis is measured along with Independent Component Analysis (ICA) for the separation of the signals. Then the distinctive features, Mel-Frequency Cepstral Coefficient(MFCC), Gamma tone-Frequency Cepstral Coefficient(GTCC) and short time energy are extracted from the acoustic signal and are trained using Neural Network(NN) classifier to identify the malicious UAV. The proposed method under different conditions outperforms the existing techniques with an accuracy of 100% in identification of malicious UAV.

Key Words: Blind Source Separation Algorithm, kurtosis, Independent Component Analysis, Mel-Frequency Cepstral Coefficient(MFCC), Gamma tone-Frequency Cepstral Coefficient(GTCC), short time energy, Neural Networks

1.INTRODUCTION

Unmanned Aerial Vehicle (UAV) technology, also known as drones, has rapidly advanced in recent years and has become an integral part of various industries and applications. UAVs are essentially aircraft that are either remotely piloted or operated autonomously without a human pilot on board. They come in various shapes and sizes, from small quadcopters to larger fixed-wing aircraft. UAVs equipped with high-resolution, thermal cameras and sensors can be used for crop monitoring, applying fertilizers and pesticides precisely, assessing the health condition of plants, search and rescue operations, providing aerial reconnaissance and locating missing persons or survivors in disaster-stricken areas, military operations, including surveillance, target acquisition, and even offensive capabilities.

Despite these numerous benefits offered by UAV technology, there are also several concerns associated with its use. Some of the main concerns include intrusion of UAVs upon people's privacy by capturing images or videos without

their consent, surveillance or data collection without proper safeguards in place, GPS spoofing attacks and Drone-based cyberattacks. The rapid proliferation of UAVs has created more challenges and opportunities for regulatory bodies to keep up with the evolving technology. Henceforth, the Governments and Aviation authorities are working to establish rules and regulations regarding flight restrictions, registration, licensing, and privacy protection, to maintain a balance between innovation and security.

In this field of identifying drones, many methods based on image, RF technology and position based techniques have been proposed. Fu et al. (2018) created a portable, SDR-based universal software radio peripheral (USRP) prototype for detecting two situations. When a drone interacts with a ground controller, it uses the cyclostationarity signature and the pseudo-Doppler concept. When a drone does not transmit a signal, a micro Doppler signature from the RF transmission is used to detect and identify it. Yang et al. (2019) proposed an improved radio frequency (RF)-based method to detect UAVs. The clutter (interference) is eliminated using a background filtering method. Then singular value decomposition (SVD) and average filtering are used to reduce the noise and improve the signal to noise ratio (SNR). Spectrum accumulation (SA) and statistical fingerprint analysis (SFA) are employed to provide two frequency estimates. These estimates are used to determine if a UAV is present in the detection environment.

Blanchard et al. (2020) presented an approach that utilizes the acoustic properties of UAVs to locate the target correctly. A pitch identification method, along with zero-phase selective bandpass filtering, is used to extract the fundamental and particular harmonics of generated sound based on its intrinsic structure. Filtering signals inside the antenna spectrum has reduced three-dimensional location errors, but localization allows for good estimations with only a few chosen harmonics. The Kalman filtering procedure is used to smooth the estimates. Anwar et al. (2019) developed a machine learning system to recognize and classify ADr sounds out of the various sounds like bird, airplanes, and thunderstorm in the noisy environment. Mel frequency cepstral coefficients (MFCC), and linear predictive cepstral coefficients (LPCC) feature extraction algorithms are implemented to extract important characteristics from ADr sound.

Min et al. (2021) designed a technique for transformer fault diagnosis by voiceprint recognition using blind source separation and a convolutional neural network. Sound samples collected from substations are evaluated for temporal and frequency domain features. A database comprising interference and transformer fault sounds has been created. The blind source separation algorithm is applied to separate interference and fault sounds. Liu et al. (2021) suggested a system that uses

a single camera to automatically identify, recognize, and track UAVs. Once identified as a UAV, the camera collects detailed images of the target location. The convolution neural network classifier trained on the dataset is used to classify images as UAV or interference such as birds. Based on the survey made, the proposed work makes use of acoustic method to detect the malicious UAVs.

2. Proposed system

The drone sounds are collected for various models and along with other environmental noises they are mixed to form the observation signal. As the first part of the work, this observation signal which contains multiple drone sounds is processed by applying Kurtosis based Independent Component Analysis (KICA) method which separates the observation signals into individual source signals. The second part is to train the system to learn to differentiate the local drone and the malicious drone. For this, the features like Mel Frequency Cepstral Coefficients (MFCC), Gamma tone Frequency Cepstral Coefficients (GTCC) and Short Time Energy (STE) are extracted from the sounds of the local drone and other drones as well the environment noises like bird sounds, traffic vehicle sounds, and aeroplane sound. Then the dataset is created and trained using neural networks. The workflow is given in Fig. 1.

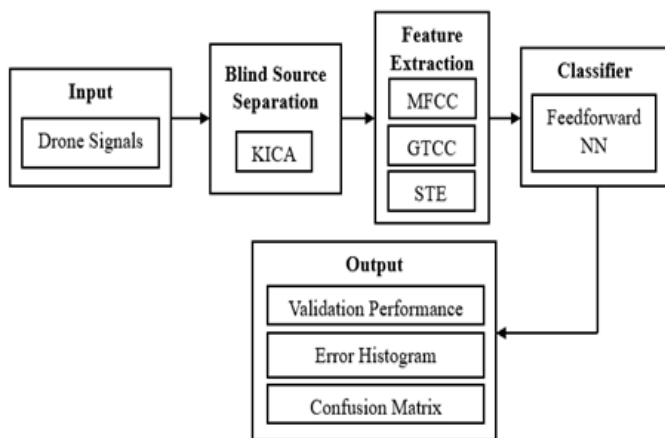


Fig -1: Block Diagram

2.1. Blind Source Separation Algorithm

Blind Source Separation (BSS) algorithms are computational methods used to separate individual source signals from a mixture of signals without prior knowledge about the sources or their characteristics. The goal of BSS is to recover the original source signals from their linearly mixed observations. BSS algorithms are particularly useful in scenarios where multiple sources are mixed together, such as in audio signal processing, image processing, and telecommunications. The underlying assumption in BSS is that the sources are statistically independent or have different statistical properties. There are several algorithms used in BSS, each with its own approach and assumptions. In this work, Kurtosis based Independent Component Analysis (KICA) method is used.

2.2. Kurtosis Based Independent Component Analysis

Kurtosis is a statistical measure that describes the shape, or "peakedness," of a probability distribution. It quantifies the degree to which a distribution deviates from the shape of a normal distribution. Kurtosis is a measure of the tail heaviness or the presence of outliers in a dataset. The KICA Algorithm is given below,

INPUT: It contains 'm' number of observation signals, where each observation signal is a mixed form of 'n' source signals.

OUPUT: The 'n' source signals obtained from the separation of observation signals.

- 1) Initially, calculate the average mean of the 'm' observation signal.
- 2) The Covariance matrix is obtained for the mean calculated observation signal matrix.
- 3) Then, the inverse of the Covariance matrix is obtained and the square root of the values of the matrix is calculated.
- 4) The centering of the data is done subtracting the mean value calculated in the first step from the observation signal matrix.
- 5) The matrix obtained from the step (4) is multiplied to the matrix obtained in step (3). The obtained dimension of the matrix will be equal to dimension of the input observation signal matrix.
- 6) The next step is to perform the Singular Value Decomposition (SVD), the obtained matrix consists of singular vectors.
- 7) Then perform the following function,

$$Z_{ica} = W(1:r,:) * Z_{cw} \quad (1)$$

Where, Z_{cw} is the result of Step 5, W is the matrix obtained after performing SVD, 'r' represents the number of independent components in the observation signal.

This type of transformation might be used for Independent Component Analysis (ICA) to separate statistically independent source signals from a mixed dataset.

2.3. Feature Extraction

In order, to train the system to identify the malicious signal, the features have to be extracted from the signals and used for training the system. The features must be chosen in such a way that they show distinct difference between the data. Generally, for audio signals, the most common features that are being extracted are Mel-Frequency Cepstral Coefficient (MFCC), Gamma tone-Frequency Cepstral Coefficient (GTCC), Short-time energy, Zero-crossing rate, pitch and spectral centroid. Among these, Mel-Frequency Cepstral Co-efficient (MFCC), Gamma tone-Frequency Cepstral Co-efficient (GTCC) and Short-time energy were chosen as they showed better distinction among the data.

2.4. Neural Network Classifier

The feedforward neural network is used to train the input features extracted from the drone signals. The trained model is then tested and validated to classify different UAVs in order to identify the malicious UAV. The performance of the network is evaluated using error histogram, validation performance and confusion matrix.

3. Results and Discussion

The proposed system was performed for the dataset obtained from the online sources and real-time data sets.

3.1. System Working for Dataset

Initially, for observing the performance of different algorithms in order to choose the better working algorithm to execute the system, the dataset of drone audio signals was obtained from the open source tool kaggle.com, Jamil et al. (2020).

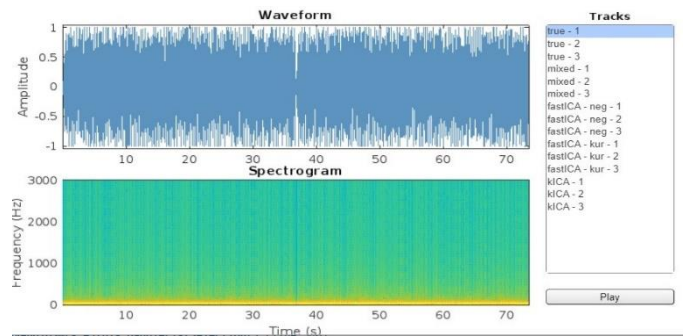
3.1.1. Ica algorithms applied to the observation signals

The performance was checked between two different ICA algorithm, FastICA using negative entropy and kurtosis and the second algorithm is using ICA based on kurtosis. Initially, three kinds of drone sounds were taken as the source signals. These source signals are named as Drone-A, Drone-B and Drone-C and their time-domain and spectrogram representation are shown in Fig. 2.

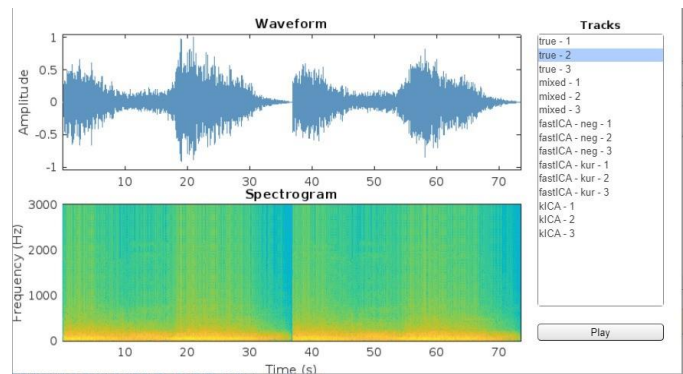
These signals were mixed to form the observation signals. The observation matrix is obtained by applying a mixing matrix to the original audio data, transforms it into a new representation using matrix multiplication, and then normalizes the transformed audio data to ensure it falls within a specific range of [-1,1]. The observation obtained for these three drone audio is shown in Fig. 3.

This observation signal was processed using the two algorithms, FastICA using negative entropy and kurtosis and ICA using Kurtosis. The following results observed are shown in Fig. 4.

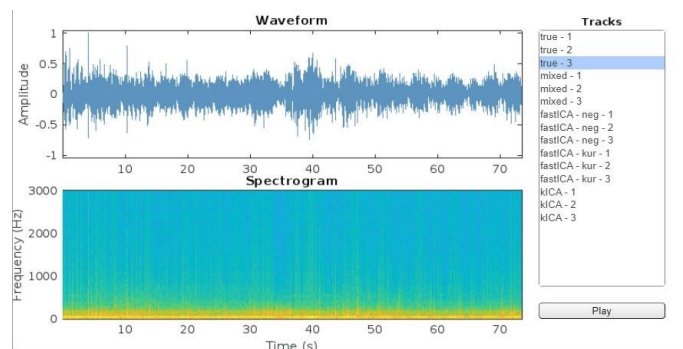
From the obtained results, comparing the time-domain and spectrogram representations of input signal of Drone-B in Fig. 2 (b) and retrieved signal of Drone-B in Fig. 4, we can infer that Kurtosis based ICA algorithm has provided better retrieval of signal than FastICA method.



(a)

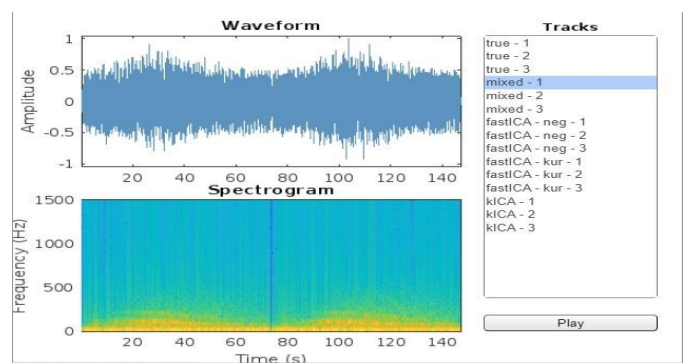


(b)

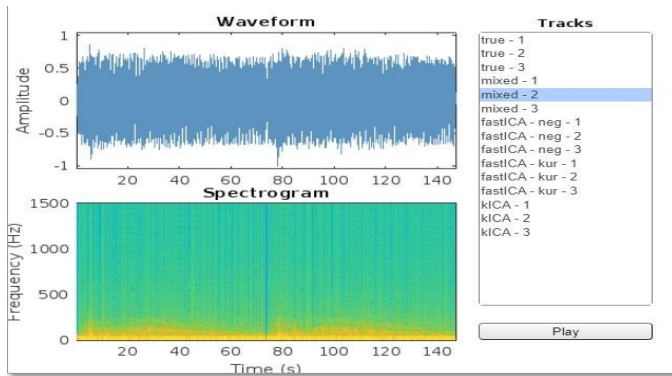


(c)

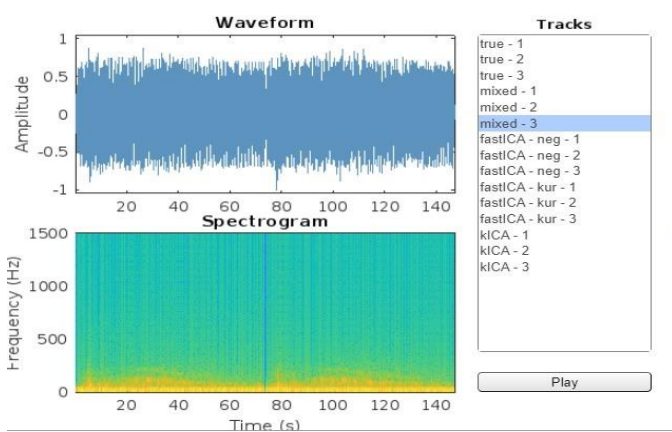
Fig -2: Time-domain and spectrogram of (a) Drone-A, (b) Drone-B and (c) Drone-C



(a)

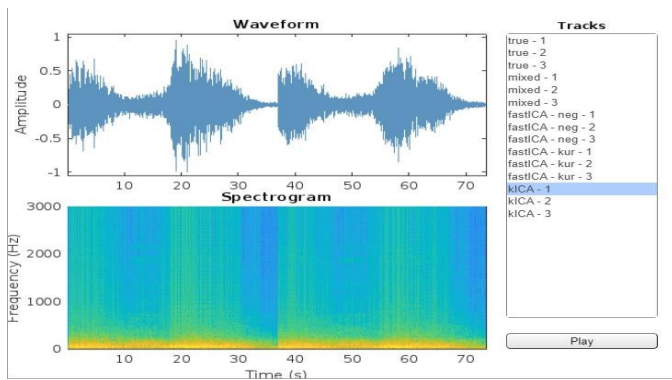


(b)

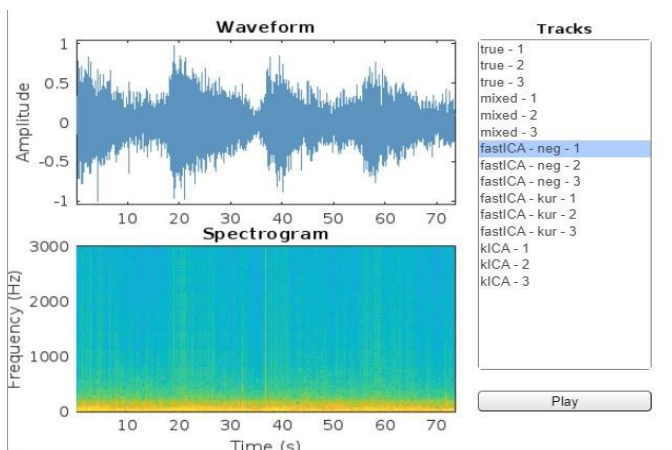


(c)

Fig -3: Time-domain and spectrogram of (a) Observation signal-1, (b) Observation signal-2 and (c) Observation signal-3



(a)

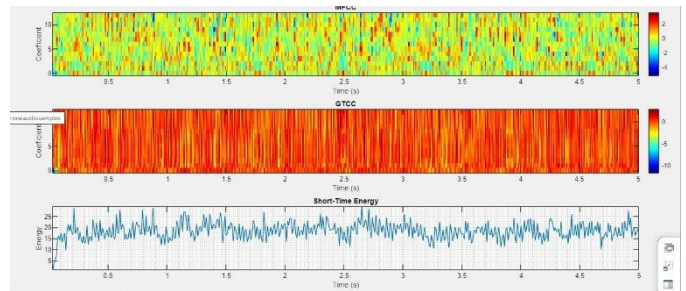


(b)

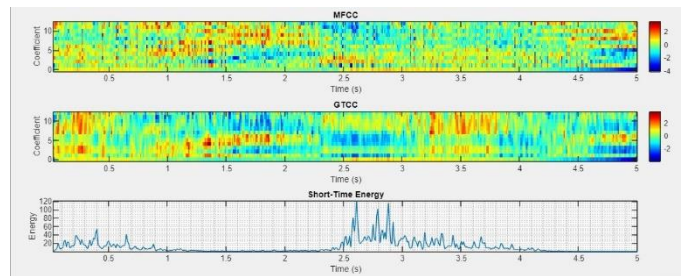
Fig -4: Time- domain and spectrogram of Retrieved signal of Drone-B using (a) KICA and (b) FastICA

3.1.2. Feature Extraction

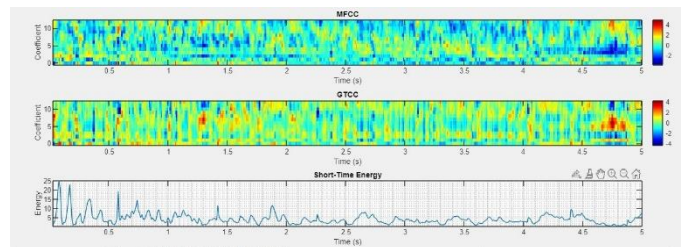
The feature extraction for all three drone audio data is shown in the Fig. 5. From the figures, it can be seen that all three features are distinct for all three signals. These signals are used for training the signals.



(a)



(b)



(c)

Fig -5: MFCC, GTCC and Short-time energy extracted for (a) Drone-A, (b) Drone-B and (c) Drone-C

3.1.3. Training using Machine Learning algorithms

For training the system, two algorithms, Support Vector Machine (SVM) and Neural Network (NN) were tested to check their performance and accuracy. The results obtained are shown in Fig. 6. From the obtained confusion matrix in SVM the accuracy level attained is 87% and that of NN is 100%. The NN has provided better classification in identifying the malicious signal than the SVM.

```

precision    recall  f1-score   support
0             0.84     1.00     0.91     3035
1             1.00     0.60     0.75     1476

accuracy          0.87     4511
macro avg         0.92     0.80     0.83     4511
weighted avg      0.89     0.87     0.86     4511

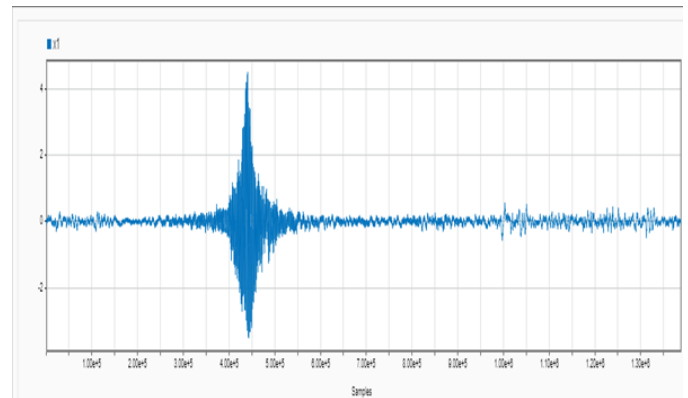
[ ] print(confusion_matrix(y_test,y_pred))

[[3035  0]
 [ 587 889]]

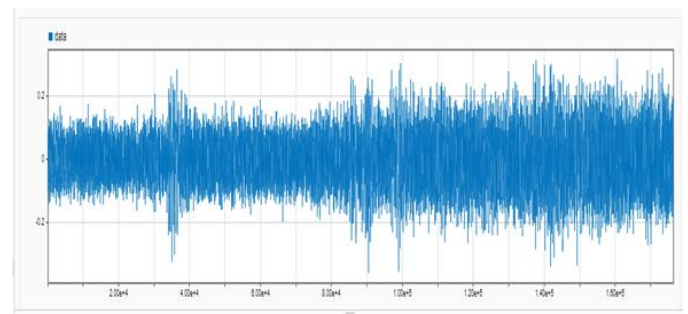
```

(a)

Table 1.

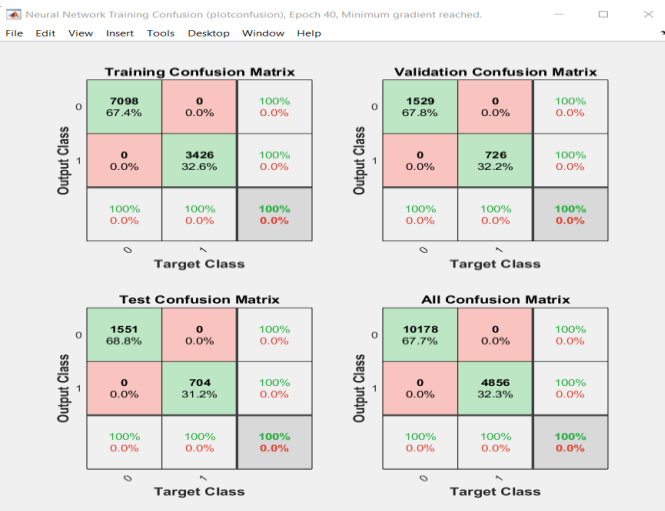


(a)



(b)

Fig -7: Time-Domain representation of (a) Fixed-Wing drone audio data and (b) Multi-Rotor audio data



(b)

Fig -6: Confusion Matrix obtained from (a) SVM and (b) Neural Networks

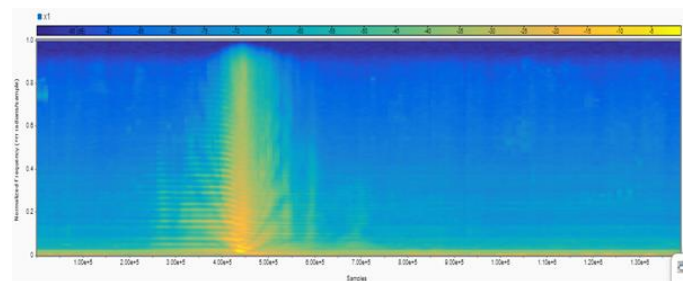
By performing the following procedures, the proposed system in Fig. 1 was framed using the algorithms that provided better results in all aspects, namely, retrieving the source signal from the observation signal, features that showed distinction among audio signals and machine learning algorithm that provided better accuracy for training the system in identifying the malicious signal.

3.2. System Performance for Real-time Data

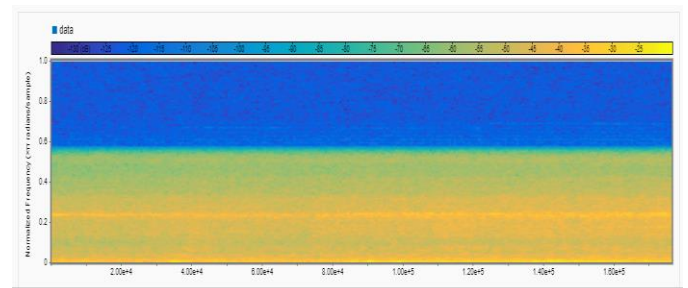
The real time dataset was collected and applied to the system to check its performance.

3.2.1. Real-Time Dataset

There are basically four types of drone- Fixed-wing, Multi-rotor, single-rotor and Hybrid drone called VTOL which is the combination of both fixed wing and multi-rotor type of drones. Out of these, Fixed-Wing drone and Multi-Rotor drone audio data was collected. The Fixed-wing drone signal was collected from Centre for Aerospace Research Remote Pilot Training Organization (CASR RPTO), MIT Campus, Anna University, Chennai. The Multi-rotor drone signal was collected from the students of Department of ECE, CEG Campus, Anna University, Chennai, which was constructed by the students for spraying the pesticides over the agriculture fields. The Time-Domain representation of Fixed-wing drone and Multi-rotor drone audio data are shown in Fig. 7 and their spectrogram are shown in Fig. 8. The signal analysis was done and its values are tabulated and shown in



(a)



(b)

Fig -8: Spectrogram of (a) Fixed –Wing drone audio data and (b) Multi-Rotor audio data

Table -1: Metrics of Fixed-wing drone signal and Multi-Rotor drone signal

Metrics	Fixed-drone signal	Multi-Rotor drone signal
Mean	5.9094e-3	-2.6858e-4
Median	-8.5449e-4	-3.6621e-4
Peak to Peak	1.7692	7.0157e-1
RMS value	2.0437e-1	6.8817e-2

Using these real-time signals, three conditions, namely, Condition 1- Fixed-Wing Drone and Multi-Rotor Drone, Condition 2- Fixed-wing Drone signal, Multi-Rotor Drone signal and Aeroplane signal, and Condition 3- Fixed-wing and Environmental noises were tested and the performance was checked. For all the three condition the Fixed-Wing was assumed to be drone signal and the other signals as malicious signal.

3.2.2. Condition 1- Fixed-Wing Drone and Multi-Rotor Drone

For the first condition, the two drone signals Fixed-wing drone audio data and the Multi-rotor drone audio data were mixed to form the observation signal and is shown in Fig. 9 and passed through the system. The observation signal is then passed through the BSS block where the separation is done using the KICA algorithm to obtain the source signal from the observation signal. From the Fig. 10, it is observed that source signal was retrieved successfully. The signal analysis was also done for retrieved signal of Fixed-wing drone and the comparison was done with the true signal values and tabulated in Table 2.

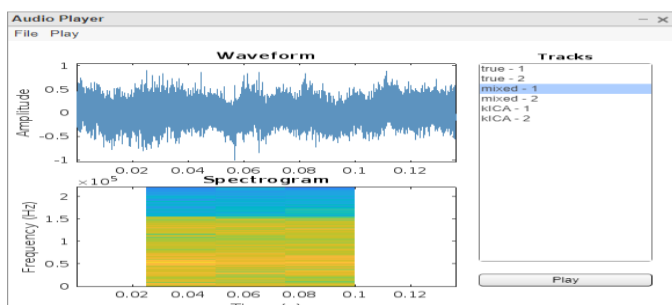


Fig -9: Observation signal for Condition-1

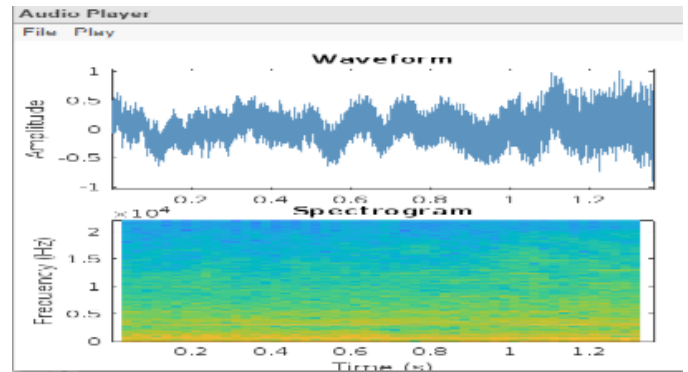


Fig -10: Retrieved Fixed-wing drone audio data after applying KICA

Table -2: Signal statistics comparison between True and Retrieved Fixed-wing drone signal

Metrics	TRUE SIGNAL	RETRIVED SIGNAL
Mean	5.9094e-3	5.8090e-3
Median	-8.5449e-4	-8.5460e-4
Peak to Peak	1.7692	1.7680
RMS value	2.0437e-1	2.0430e-1

From the Table 2, we can infer that the true and retrieved signal statistics lies in almost equal range and hence we can say that the retrieval has been done properly. Next, the features MFCC, GTCC and Short-Time Energy are extracted from the retrieved signal to train the signal using Neural Networks. The number of samples taken for training, validation and testing and its cross entropy and error percentage is shown in Fig. 11. The validation performance graph show the error rate at each epoch being performed as shown in Fig. 12. At the end of maximum epoch when the model is trained to identify the malicious signal the error rate must be low, this denotes the best working model. From Fig. 12, it is inferred that the graph is in the decaying fashion and at the end of the 28th epoch the error rate at the minimum level and the performance value is 7.3053e-07. The error histogram graph for Condition 1 in Fig. 13 shows that the error range for maximum samples lies between -1.9e-07 and 2.49e-07 and they lie close to the zero error mark which implies minimum error. The confusion matrix in Fig. 14 shows how well the model has been trained in classifying between the signals. Among 267 samples, the model has properly classified 133 Fixed-wing drone signals as local drone signals and remaining 134 Multi-Rotor drone signals as malicious signals without any miss classification. The accuracy can be found by the formula,

$$\text{Accuracy} = (TP + TN)/(TP+TN+FP+FN) \quad (2)$$

After applying in the above formula, the accuracy level obtained is 100%.

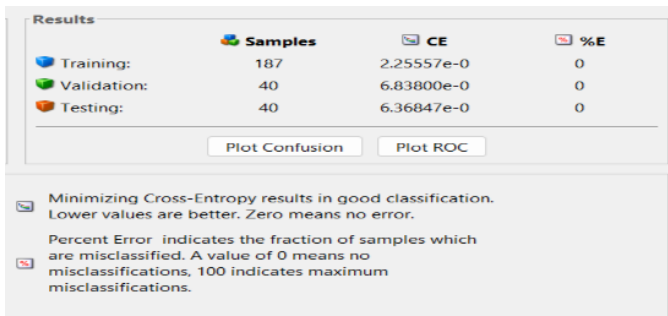


Fig -11: Number of samples taken for testing, validation and testing along with the cross entropy and percentage of error for Condition 1

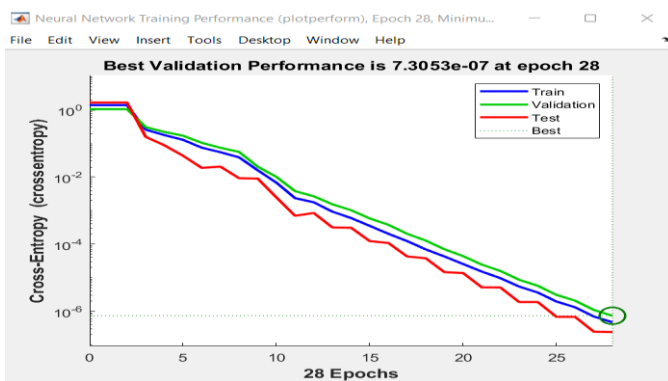


Fig -12: Validation Performance for condition 1

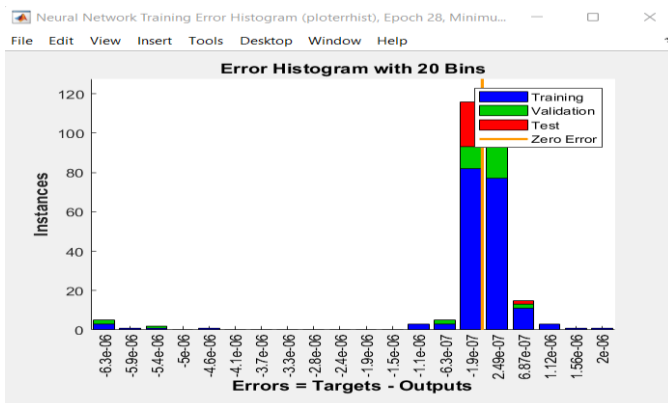


Fig -13: Error Histogram for Condition 1

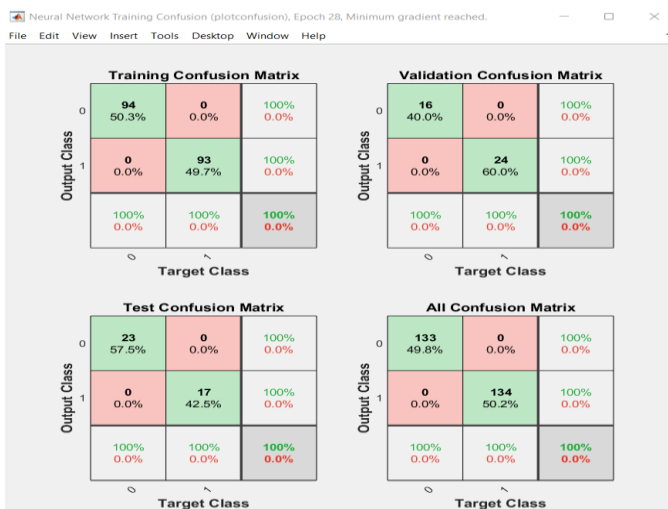


Fig -14: Confusion Matrix for Condition 1

From the condition 1 being performed, the system was able to separate the source signal from the observation signal,

the features were extracted and applied to train the model and the accuracy obtained was 100%. In this condition the system classified the malicious signal successfully.

3.2.3. Condition 2- Fixed-wing Drone signal, Multi-Rotor Drone signal and Aeroplane signal

For the second condition, three kinds of signals were considered, Fixed-wing drone audio, Multi-Rotor drone audio and Aeroplane drone audio. Since the fixed-wing is developed based on the model of airplane, this condition is being done to check whether the KICA algorithm performs well in separating these signals successfully. The observation signal and the retrieved signal obtained are shown in Fig. 15 and 16.

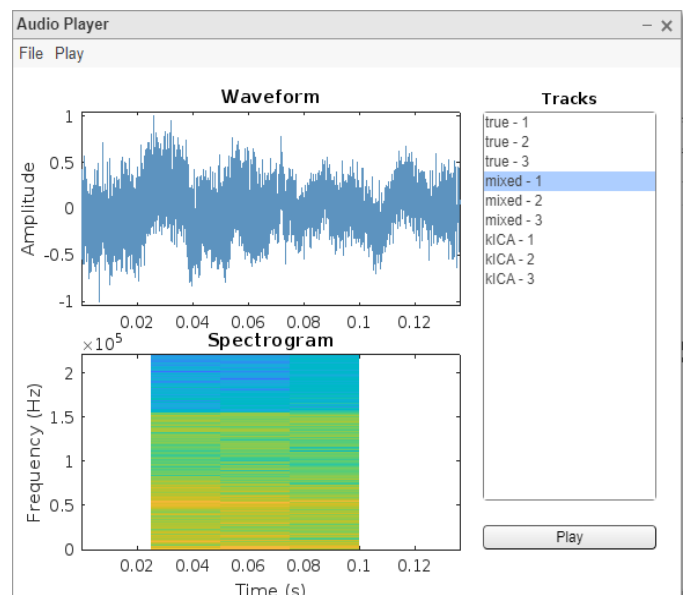


Fig -15: Observation signal for Condition 2

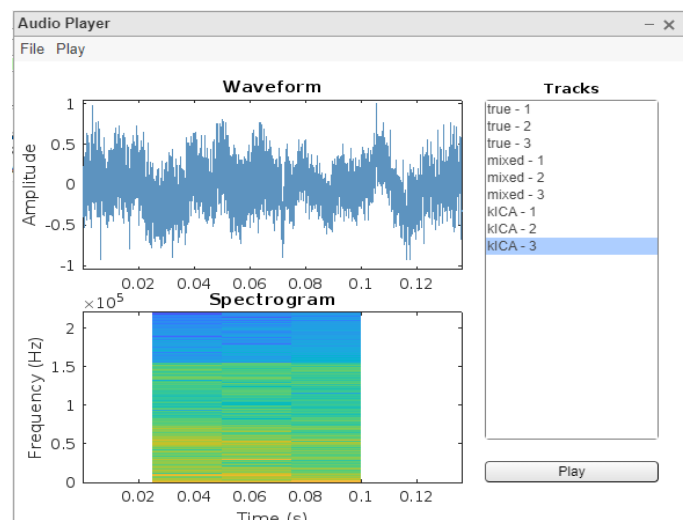


Fig -16: Retrieved Fixed-wing drone audio data after applying KICA

From the comparison of the True signal of fixed-wing in Fig. 7 (a) and Fig. 8 (a) with the retrieved signals in Fig. 16, it shows that the retrieving is not completely done. Then the signal analysis is done for retrieved Fixed-Wing signal and the comparison is done with the true signal and is tabulated in Table 3.

Table -3: Signal statistics comparison between True and Retrieved Fixed-wing drone signal

Metrics	TRUE SIGNAL	RETRIEVED SIGNAL
Mean	5.9094e-3	-1.5261e-5
Median	-8.5449e-4	3.5095e-3
Peak to Peak	1.7692	1.9290
RMS value	2.0437e-1	2.3884e-1

From the Table 3, it is observed that there is slight variation in the true and retrieved signal statistics as the retrieval of source signal is not completely done. Next, the features MFCC, GTCC and Short-Time Energy are extracted from the retrieved signal to train the signal using Neural Networks. The number of samples taken for training, validation and testing and its cross entropy and error percentage is shown in Fig. 17. The validation performance graph for the condition 2 is shown in Fig. 18. It shows that the model has taken 27 epochs to reach the minimum error rate of 1.0222 e-05. The error histogram for condition 2 in Fig. 19, shows that the error range is -1.1 e-05 which lies very much close to the zero error line. This is very much closer than the condition1 error range value. The confusion matrix for condition 2 obtained is shown in Fig. 20. The model has classified 268 samples of Fixed drone signals as local drone signals and the remaining 134 samples of malicious signals i.e aeroplane signal and multi-rotor signal in condition 2 as malicious without any misclassification.

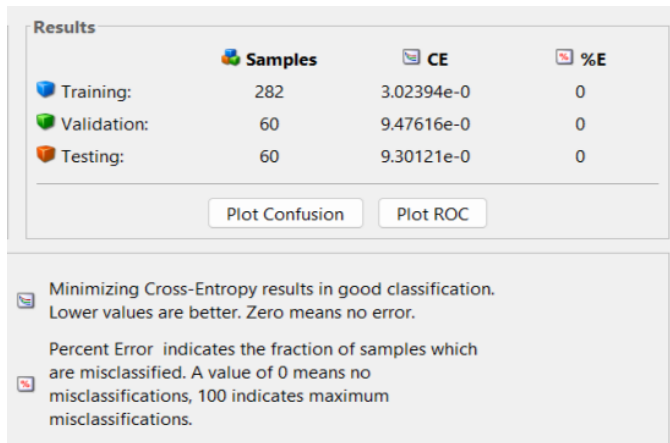


Fig -17: Number of samples taken for training, validation and testing along with the cross entropy and percentage of error for Condition 2

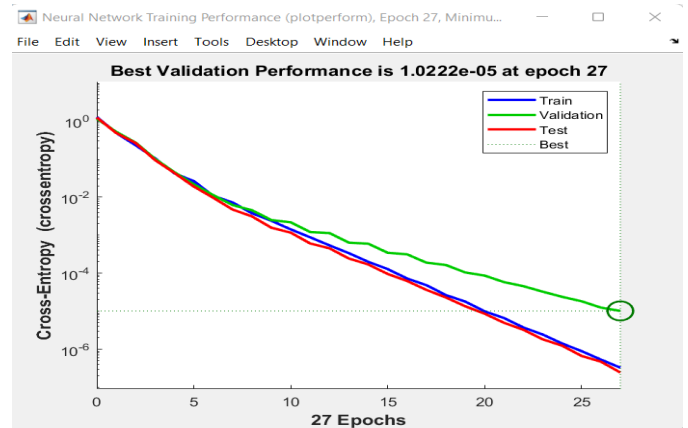


Fig -18: Validation Performance for condition-2

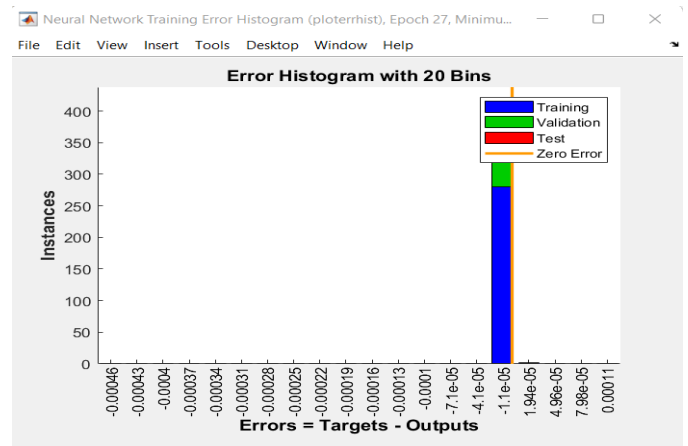


Fig -19: Error Histogram for Condition2



Fig -20: Confusion Matrix for Condition 2

From condition 2, the KICA algorithm performance was not as expected. Since the aeroplane signal was similar to Fixed-wing drone signal and the kurtosis was based on peakness calculation, the retrieval of signal was little hard. But still, the training of the model in classifying the signal between drone and malicious was done perfectly as the features being extracted was distinct.

3.2.4. Condition 3 – Fixed –wing and Environmental noises

In condition 3, the Fixed-wing drone audio with environment sounds like traffic sound and bird sound were taken. The observation signal for these three signal and the retrieved signal of Fixed-Drone signal are shown in Fig. 21 and 22. The signal statistics was calculated for the retrieved Fixed-wing signal and compared with the true signal and its tabulated in Table 4.

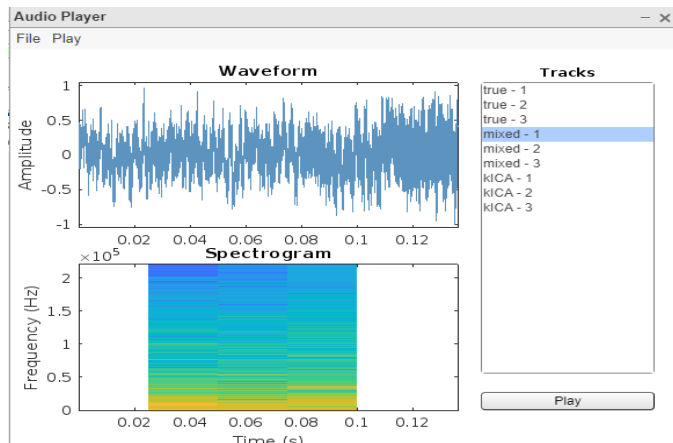


Fig -21: Observation signal for Condition 3

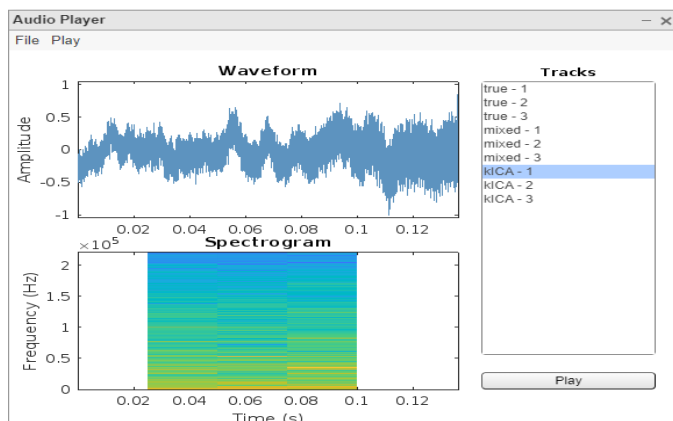


Fig -22: Retrieved Fixed-wing drone audio data after applying KICA

Table -4: Signal statistics comparison between True and Retrieved Fixed-wing drone signal

Metrics	TRUE SIGNAL	RETRIVED SIGNAL
Mean	5.9094e-3	-1.5237e-5
Median	-8.5449e-4	5.6915e-3
Peak to Peak	1.7692	1.8431
RMS value	2.0437e-1	2.0067e-1

From the Table 4, it is observed that the true and retrieved signal statistics have variation in their values.

Thereby it implies that the retrieval of source signal is not done completely as that of condition 2. Next, the features MFCC, GTCC and Short-Time Energy are extracted from the retrieved signal to train the signal using Neural Networks. The number of samples taken for training, validation and testing and its cross entropy and error percentage is shown in Fig. 23. The validation performance graph for the condition 3 in Fig. 24 shows that the model has taken 26 epochs to reach the minimum error rate of 3.0532e-07. The error histogram for condition 3 is shown in Fig. 25, from which it is inferred that the error range in which the maximum samples of training, validation and testing lies is -9.3 e-06. For this, the zero error line lies in the error range. This infers that system has performed better for this condition. The confusion matrix for condition 3 is shown in Fig. 26.

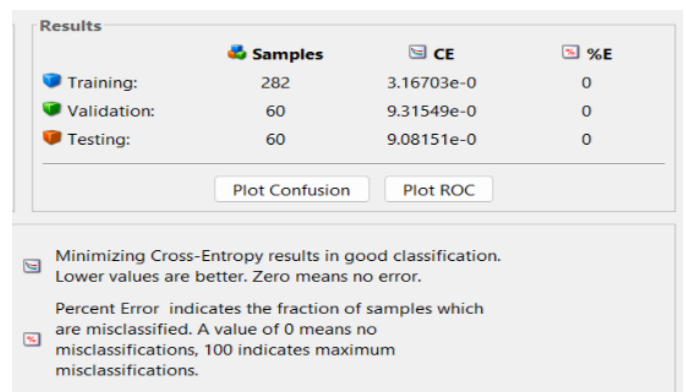


Fig -23: Number of samples taken for training, validation and testing along with the cross entropy and percentage of error for Condition 3

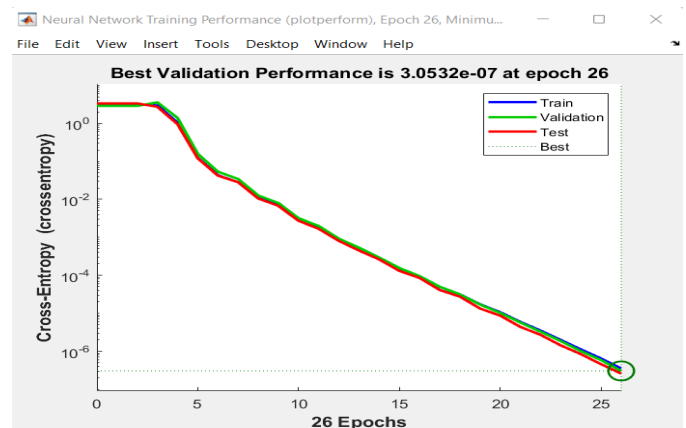


Fig -24: Validation Performance for condition 3

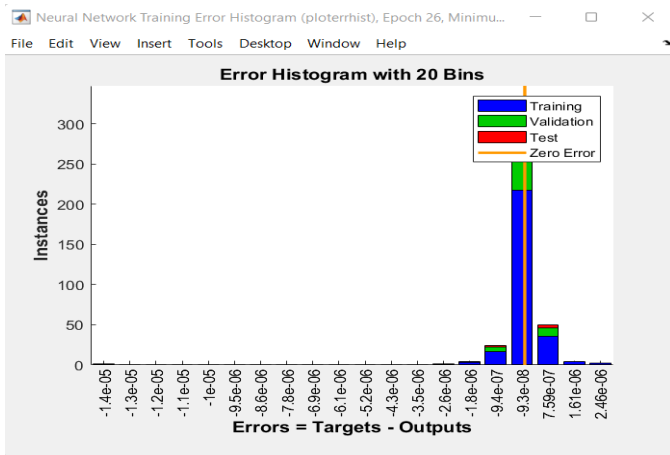


Fig -25: Error Histogram for Condition 3

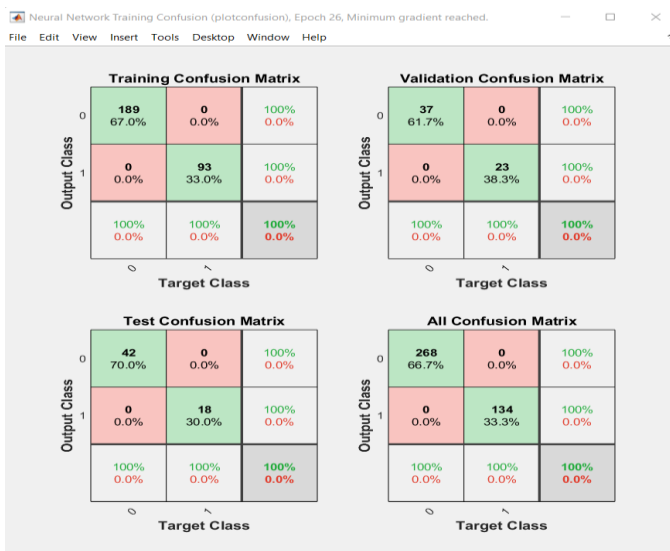


Fig -26: Confusion Matrix for Condition 3

Thus, the model has classified 268 samples of Fixed drone signals as local drone signals and the remaining 134 samples of malicious signals i.e. traffic car signal and bird sound as malicious without any misclassification as features considered were distinct.

4. CONCLUSION

In this work, the objective was to identify the malicious drone that enters the secured perimeter. The BSS algorithm, KICA was performed on the collected drone signals which efficiently separated the source signals from the observation signal. The NN classifier was trained with extracted features and then tested and validated for three different conditions. For the condition 1 – Fixed wing and Multi Rotor and for condition 3 – Fixed wing drone audio and external noises, the KICA algorithm separated the source signal from the observation signal with high similarities. In case of condition 2 – Fixed wing drone audio, Multi-rotor drone audio and airplane audio, the KICA retrieved the source signal with a small amount of disturbance. The training, testing and validation of the model were done with 100% accuracy for all three conditions but the difference occurs in number of epochs it underwent for successful training and the error range for all three conditions. The number of epochs for first condition where it reached minimum error rate of 7.3053e-07 is 28

epochs. For condition 2, the minimum error rate of 3.27e-07 was reached at 27th epoch. Similarly, for third condition, the minimum error rate of 3.0532e-07 was reached at 26th epoch.

ACKNOWLEDGEMENT

This study was supported by Centre for Aerospace Research Remote Pilot Training Organization (CASR RPTO), MIT Campus, Anna University, Chennai and Department of ECE, CEG Campus, Anna University, Chennai.

REFERENCES

- Anwar, M. Z., Kaleem, Z., & Jamalipour, A. (2019). Machine learning inspired sound-based amateur drone detection for public safety applications. *IEEE Transactions on Vehicular Technology*, 68(3), 2526-2534.
- Blanchard, T., Thomas, J. H., & Raouf, K. (2020). Acoustic localization and tracking of a multi-rotor unmanned aerial vehicle using an array with few microphones. *The Journal of the Acoustical Society of America*, 148(3), 1456-1467.
- Ding, S., Huang, J., Wei, D., & Cichocki, A. (2006). A near real-time approach for convolutive blind source separation. *IEEE Transactions on Circuits and Systems I: Regular Papers*, 53(1), 114-128.
- Douglas, S. C., Gupta, M., Sawada, H., & Makino, S. (2007). Spatio-Temporal FastICA algorithms for the blind separation of convolutive mixtures. *IEEE transactions on audio, speech, and language processing*, 15(5), 1511-1520.
- Fu, H., Abeywickrama, S., Zhang, L., & Yuen, C. (2018). Low-complexity portable passive drone surveillance via SDR-based signal processing. *IEEE Communications Magazine*, 56(4), 112-118.
- Gan, Y., Li, W., Zheng, Z., Zhao, J., Zou, K., & Cai, B. (2021). Cognitive Radar Signal Processing Based on Convolutional Neural Network. In *2021 IEEE 6th International Conference on Signal and Image Processing (ICSIP)* (pp. 784-789). IEEE.
- Ghani, S. H., & Khan, W. (2020). Extraction of UAV sound from a mixture of different sounds. *Acoustics Australia*, 48(3), 363-373.
- Gupta, S., Jaafar, J., Ahmad, W. W., & Bansal, A. (2013). Feature extraction using MFCC. *Signal & Image Processing: An International Journal*, 4(4), 101-108.
- Jamil, S., Abbas, M. S., & Roy, A. M. (2022). Distinguishing malicious drones using vision transformer. *AI*, 3(2), 260-273.
- Jamil, S., Fawad, Rahman, M., Ullah, A., Badnava, S., Forsat, M., & Mirjavadi, S. S. (2020). Malicious UAV detection using integrated audio and visual features for public safety applications. *Sensors*, 20(14), 3923.
- Liu, Y., Liao, L., Wu, H., Qin, J., He, L., Yang, G., ... & Zhang, J. (2021). Trajectory and image-based detection and identification of UAV. *The Visual Computer*, 37, 1769-1780.
- McKenzie, T., Dagleish, F., Vuorenkoski, A., Ouyang, B., Britton, W., Ramos, B., & Shirron, J. (2018). Simulation and experiment waveform comparison for undersea pulsed laser in application to target localization. In *OCEANS 2018 MTS/IEEE Charleston* (pp. 1-7). IEEE.
- Min, L., Huamao, Z., & Annan, Q. (2021). Voiceprint recognition of transformer fault based on blind source separation and convolutional neural network. In *2021 IEEE Electrical Insulation Conference (EIC)* (pp. 618-621). IEEE.
- Rong, Y., Nordholm, S., & Duncan, A. (2021). On the capacity of underwater optical wireless communication

- systems. In 2021 Fifth Underwater Communications and Networking Conference (UComms) (pp. 1-4). IEEE.
15. Scholz, T. (2018). Laser based underwater communication experiments in the Baltic Sea. In 2018 Fourth Underwater Communications and Networking Conference (UComms) (pp. 1-3). IEEE.
 16. Sheu, B. H., Chiu, C. C., Lu, W. T., Huang, C. I., & Chen, W. P. (2019). Development of UAV tracing and coordinate detection method using a dual-axis rotary platform for an anti-UAV system. *Applied Sciences*, 9(13), 2583.
 17. Thomas, J., Deville, Y., & Hosseini, S. (2006). Time-domain fast fixed-point algorithms for convolutive ICA. *IEEE Signal Processing Letters*, 13(4), 228-231.
 18. Uddin, Z., Altaf, M., Bilal, M., Nkenyereye, L., & Bashir, A. K. (2020). Amateur Drones Detection: A machine learning approach utilizing the acoustic signals in the presence of strong interference. *Computer Communications*, 154, 236-245.
 19. Wang, W., Fan, K., Ouyang, Q., & Yuan, Y. (2022). Acoustic UAV detection method based on blind source separation framework. *Applied Acoustics*, 200, 109057.
 20. Yan, Z., Sheng-kai, S., Yue, L., & Jia-qi, W. (2020). Sonar echo signal processing based on Convolution Blind source separation. In 2020 IEEE 3rd International Conference on Information Communication and Signal Processing (ICICSP) (pp. 130-134). IEEE.
 21. Yang, S., Qin, H., Liang, X., & Gulliver, T. A. (2019). An improved unauthorized unmanned aerial vehicle detection algorithm using radiofrequency-based statistical fingerprint analysis. *Sensors*, 19(2), 274.
 22. Yang, Y., Li, Z., Wang, X., & Zhang, D. (2011). Noise source separation based on the blind source separation. In 2011 Chinese Control and Decision Conference (CCDC) (pp. 2236-2240). IEEE.
 23. Yin, H. S., Zhang, P., Qian, J. S., & Hua, G. (2009). Feature extraction and recognition of ventilator vibration signal based on ICA/SVM. In 2009 2nd International Congress on Image and Signal Processing (pp. 1-4). IEEE.
 24. Zheng, S., Cao, X., Tong, F., Zhang, G., & Dong, Y. (2018). Performance evaluation of acoustic network for underwater autonomous vehicle in confined spaces. In 2018 IEEE 8th International Conference on Underwater System Technology: Theory and Applications (USYS) (pp. 1-4). IEEE.